

## ANALYTICAL PWR VESSEL INTEGRITY ASSESSMENT BY TEARING INSTABILITY THEORY

J. R. TARPANI and D. SPINELLI

*Department of Materials Engineering, Engineering School of Sao  
Carlos, Av. Dr. Carlos Botelho, 1465, Sao Carlos, Brazil*

### ABSTRACT

Analytical failure predictions for a PWR vessel from Linear Elastic and Elastic-Plastic Fracture Mechanics have been compared. Results were related to internal pressure and wall thickness strain gradient. The conservatism of linear elasticity via  $K_{IC}$  when compared to elasto-plasticity by means of the Ductile Tearing Instability Theory was quantified. The overriding effect of testpiece size on both approaches as well as of side-grooving on elasto-plasticity were shown. The healthy conservatism of the  $J_{50}$  criterion for design and service was demonstrated and the J-R curve linear extrapolation on J-T space as well. The ductile crack extensions undergone by the nuclear component were calculated according to several elastic-plastic criteria. On these bases, some considerations about leak-before-break were made. Finally, the logarithmic fit for J-R curves was proposed.

### KEYWORDS

J-R curve, leak-before-break, PWR vessel failure, safe design and service, structural integrity, tearing instability.

### INTRODUCTION

The undue conservatism in the instability evaluation of structural components under upper-shelf conditions via Linear Elastic Fracture Mechanics (LEFM) criteria as compared to Elastic-Plastic Fracture Mechanics (EPFM) methodologies is widely recognized. Nevertheless this quantification has never been properly appreciated. Specifically, the linear elastic criterion,  $K_{IC}$  for cleavage triggering, is always applied on PWR assessment. Not willing to underestimate its importance in pressurized thermal shock studies, it seems interesting to estimate the predictions of instability according to  $K_{IC}$  when the system operates under fully ductility response and then compare them quantitatively to those more realistic from Elastic-Plastic Tearing Instability Theory (J-T diagrams). In this work, such analytical comparison is accomplished for a PWR vessel considering eight different cracks types. The results are helpful for hydrotesting purposes.

## MATERIAL, SPECIMENS TEST AND STRUCTURAL COMPONENT

A 130 mm thick nuclear forged plate steel, grade A508-3A, was tested in the as-received condition. This material exhibited a yield strength,  $S_Y$ , of 384 MPa, a ultimate tensile strength,  $S_U$ , of 519 MPa when tested at 175°C. One and two inch-thick proportional-compact specimens for K and J toughness testing were extracted from the central portion of the plate in the ST orientation. The cylindrical PWR vessel, with mean radius,  $R$ , of 950 mm and wall thickness,  $t$ , of 130 mm is shown in scheme in Fig.1. The vessel is supposed to have four elliptical embedded cracks (with nil eccentricity) and four semi-elliptical cracks in the outside surface wall (each one individually considered) which are fully submitted to the hoop stresses. The component is internally pressurized at 175°C.

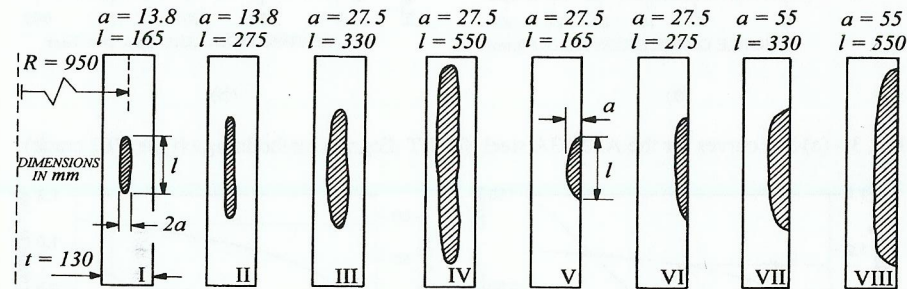


Fig.1 - Eight axial cracks in the belt-line of a intermediate size PWR vessel.

## EXPERIMENTAL AND ANALYTICAL PROCEDURES

## Linear Elastic Fracture Mechanics (LEFM)

$K_{IC}$  tests were carried out according to ASTM-399 standard (1995) at temperatures from -196°C to -60°C in order to achieve maximum valid  $K_{IC}$  results for both specimen sizes. The stress intensity K factor for a surface crack with depth  $a$  ( $2a$  for internal cracks) axially sited in the belt-line of a cylindrical isothermally pressurized vessel is given by the ASME code (1992):

$$K_{IM} = S_M \cdot M_M \sqrt{\frac{\pi \cdot a}{Q}} \quad (1)$$

where  $K_{IM}$  points out the mode I loading,  $S_M$  is the nominal hoop membrane stress and  $M_M$  and  $Q$  are crack shape factors. In elastic regime, K is related to J-integral by:

$$J = \frac{K_I^2}{E'}, \text{ where } E' \begin{cases} E & (\text{plane-stress}) \\ E / (1 - \nu^2) & (\text{plane-strain}) \end{cases} \quad (2)$$

$E$  and  $\nu$  are material constants. From (1) in (2) and introducing the yield strength ( $S_Y$ ):

$$J_{APP} = \frac{S_Y^2 \cdot a}{E'} \cdot \left\{ \frac{S_M^2 \cdot \pi}{S_Y^2} \right\} \left[ \frac{M_M^2}{Q} \right] \quad (3)$$

where the symbols  $\{ \}$  and  $[ \ ]$  are respectively stress and geometric correction terms.  $J_{APP}$  is implicitly related to the internal pressure,  $P$ , in Eq.3 by means of  $S_M$ . The strain gradient vessel wall-through, with respect to  $P$  and  $S_M$ , was obtained from thick-walled components theory and Ramberg-Osgood law. The  $J_{APP} \times P \times e_M$  diagrams were constructed, where  $e_M$  is the maximum,  $e_{M(MAX)}$ , and minimum,  $e_{M(MIN)}$ , nominal hoop strain, and after introducing the converted  $J_{MAT}$  values of material cracking resistance in terms of J-integral (Eq.2), the predictions for the vessel failure by elasticity theory upon  $K_{IC}$  criterion were achieved.

## Elastic Plastic Fracture Mechanics (EPFM)

J-R curves were obtained at 175°C for 8% and 21% side-grooved specimens using the recently developed linear normalization technique (Reese and Schwalbe, 1993) in accordance with ASTM-E1152 standard (1995). The J-R data points were adjusted by both power law and logarithmic fits. Following J-T diagrams methodology (Paris and Johnson, 1983), where T is the tearing modulus, and deriving J-R curves, the  $J-T_{MAT}$  curves were obtained, where  $T_{MAT}$  is the increase rate on the material cracking resistance. The loading curves for the cracked structure,  $J-T_{APP}$ , where  $T_{APP}$  is the increase rate on the crack driving force, were achieved by:

$$\frac{J_{APP}}{T_{APP}} = \frac{S_Y^2 \cdot a}{E} \quad (4)$$

At the intersection of  $J-T_{MAT}$  and  $J-T_{APP}$  curves, that is, when  $T_{MAT}$  equals  $T_{APP}$ :

$$\frac{dJ_{MAT}}{d\Delta a} \cdot \frac{E}{S_Y^2} = T_{MAT} = T_{APP} = \frac{dJ_{APP}}{da} \cdot \frac{E}{S_Y^2} \quad (5)$$

the J values for the vessel instability ( $J_{inst}$ ) were determined. The so called  $J_{50}$  values, suggested as a good approximation of  $J_{inst}$ , were obtained from a loading curve given by  $J/T_{MAT} = 50$  lbf/in = 8.8 kJ/m<sup>2</sup>. The  $J_i$  values of ductile tearing initiation (ASTM-E813 standard, 1995) were determined from 0.2 mm off-set criterion. The instability predictions according to  $J_{50}$  and  $J_{inst}$  were settled as intervals with the upper and lower limits related to respectively to  $J-T_{MAT}$  curves fitted by power law and linear extrapolation based on  $\omega$  criterion of Deformation-J ( $\omega = 5$  for CT[S]). The  $J_{APP}$  values (Eq.3) on plastic range were calculated by considering an intermediate condition between plane stress and plane strain for the stress correction, while the geometrical solutions were supplied by the ASME code (1992). Just as for the LEFM analysis,  $J_{APP} \times P \times e_M$  diagrams were traced and also the vessel failure predictions, in terms of internal pressure and strain gradient, were determined for all elastic-plastic criteria and crack types.

## RESULTS AND DISCUSSION

Figure 2(a) presents the results of fracture toughness testing, K, when one valid result was obtained from 2TCT specimens and two from 1TCT ones. A  $K_{IC}$  curve was drawn according to

ASME code (1992) for the reference temperature (RTndt, for a Charpy specimen lateral expansion of 0.9 mm) of the A508-3A steel. This curve is shown to be conservative when compared to the 2TCT specimen valid result and slightly unconservative with respect to the less massive 1TCT specimens results. Figure 2(b) shows the graphical procedure on obtaining the critical values of the vessel failure upon  $K_{IC}$ .

Figure 3(a) presents the J-R curves for 1T and 2TCT side-grooved specimens. In both approaches, LEFM and EPFM, the massive specimens 2TCT provided the most realistic (and liberal) results, since the specimen width was almost identical to the vessel wall thickness, allowing simulation of axial cracks growing on radial direction. So, their results were used for instability analysis. In addition, 21% side-grooving of J specimens gross thickness produced almost perfectly straight crack fronts (slightly inverted tunneling) and very small thickness changes, as expected to occur in PWR vessels due to highly constrained yielding. This way, 2TCT 21% SG specimen results were applied to EPFM analysis. In Fig. 3(a) it is also observed the best pliability of the logarithmic (against power law) fit adjusting the J-R data points for high crack extension levels, where J-saturation takes place and the ductile instability is of main concern. In Fig. 3(b), in the J-T space for crack stability analysis, the  $J-T_{MAT}$  curves (dotted line for J-R logarithmic fit) of material tearing resistance relatively to 2TCT 21% SG specimen, and the  $J-T_{APP}$  curves (straight lines) of  $J_{50}$  criterion and mechanical loading (pressurization) considering type VIII crack are plotted.  $J_{50}$  and  $J_{inst}$  values (upper limits) are indicated for the  $J-T_{MAT}$  curve derived from J-R power law fit.

The extended stress correction factor and the Ramberg-Osgood law for the A508-3A steel at 175°C are presented in Fig. 4(a). Figure 4(b) shows the graphical procedure to determine failure conditions according to elastic-plastic criteria. All the failure predictions upon both LEFM and EPFM methodologies are presented in Table I. Back to the Fig. 3(a) and based on the J-R curve referred to 2TCT 21% SG testpiece it was possible to achieve the ductile crack growth levels ( $\Delta a$ ) before the vessel failure upon EPFM criteria, as specified in Table II.

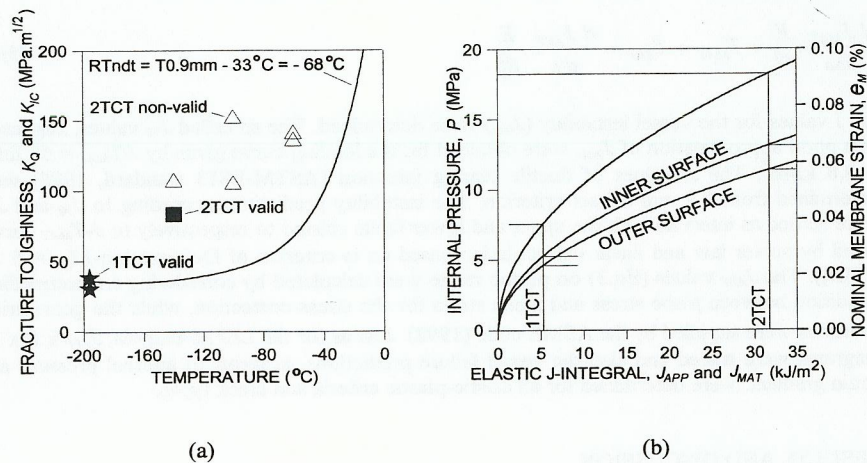


Fig. 2 - (a) Fracture toughness,  $K_Ic$ , results (valid  $K_{IC}$ , non-valid  $K_0$ ) for the A508-3A steel; (b) Pressure and strain failure predictions upon  $K_{IC}$  criterion (considering the presence of the type VIII crack).

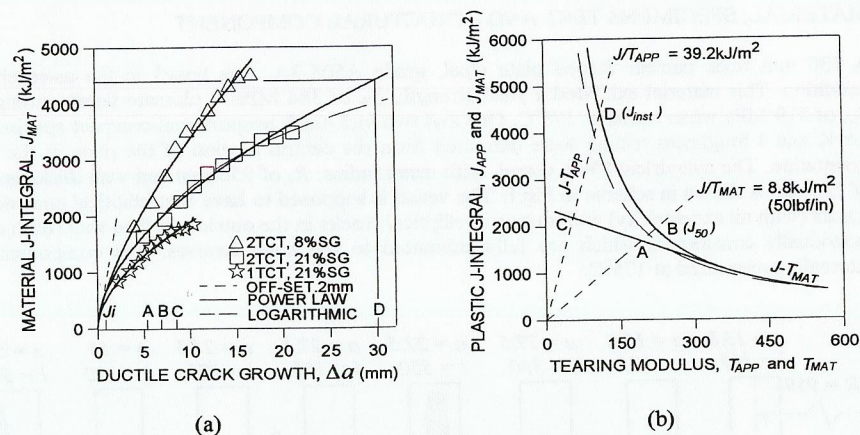


Fig. 3 - (a) J-R curves for the A508-3A steel; (b) J-T diagram methodology (type VIII crack).

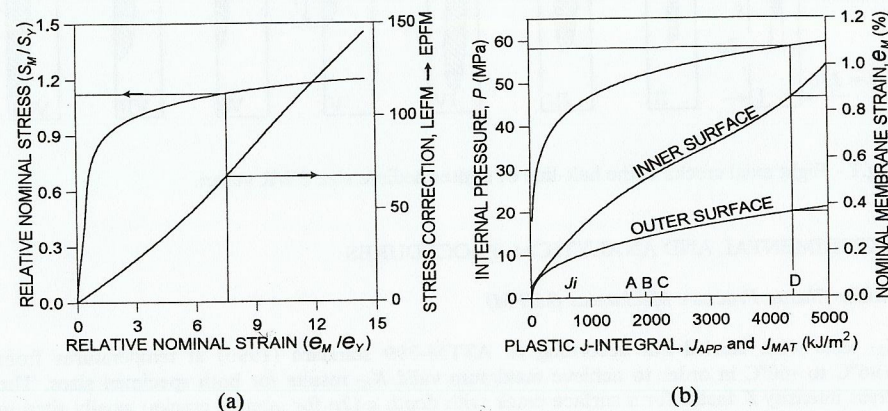


Fig. 4 - (a) Ramberg-Osgood law and the elastic-plastic stress factor for the A508-3A steel; (b) Pressure and strain failure predictions for the pressure vessel based on EPFM (type VIII crack).

Table I - PWR vessel failure predictions following LEFM and EPFM analyses.

CRACK TYPE	CRITERION	P (MPa)	$e_{M(MAX)}$ (%)	$e_{M(MIN)}$ (%)
I	$K_{IC}$	55.4	0.80	0.30
	$J_i$	57.5	1.19	0.35
	$J_{50}$	63.7-65.7	2.42-3.02	0.68-0.84
	$J_{inst}$	63.9-65.8	2.50-3.15	0.70-0.89

Table I (cont.)

CRACK TYPE	CRITERION	P (MPa)	$e_{M(MAX)}$ (%)	$e_{M(MIN)}$ (%)
II	$K_{IC}$	54.2	0.69	0.27
	$J_i$	57.1	1.16	0.34
	$J_{50}$	63.5-65.5	2.38-2.96	0.65-0.82
	$J_{inst}$	63.8-65.7	2.43-3.05	0.69-0.87
III	$K_{IC}$	36.0	0.14	0.12
	$J_i$	51.5	0.61	0.26
	$J_{50}$	58.3-59.4	1.35-1.52	0.47-0.51
	$J_{inst}$	59.7-62.6	1.56-2.18	0.52-0.65
IV	$K_{IC}$	35.3	0.13	0.11
	$J_i$	51.3	0.60	0.25
	$J_{50}$	58.2-59.3	1.30-1.47	0.46-0.50
	$J_{inst}$	59.5-62.5	1.51-2.12	0.51-0.64
V	$K_{IC}$	37.4	0.14	0.12
	$J_i$	52.9	0.65	0.27
	$J_{50}$	59.7-60.5	1.49-1.65	0.49-0.54
	$J_{inst}$	61.1-63.4	1.73-2.39	0.56-0.68
VI	$K_{IC}$	34.0	0.12	0.105
	$J_i$	50.9	0.55	0.23
	$J_{50}$	57.6-58.7	1.21-1.35	0.42-0.46
	$J_{inst}$	59.2-61.7	1.42-1.97	0.47-0.61
VII	$K_{IC}$	22.6	0.09	0.07
	$J_i$	46.0	0.32	0.21
	$J_{50}$	52.9-54.0	0.66-0.74	0.31-0.33
	$J_{inst}$	54.8-60.3	0.80-1.35	0.34-0.46
VIII	$K_{IC}$	18.5	0.065	0.06
	$J_i$	43.6	0.22	0.17
	$J_{50}$	50.7-51.8	0.48-0.51	0.25-0.27
	$J_{inst}$	52.7-58.5	0.55-0.87	0.28-0.37

Table II - Ductile crack growth (in millimeters, and for each one crack fronts) preceding the failure of the pressure vessel according to elastic-plastic analysis for the eight crack types.

CRITERION	I	II	III	IV	V	VI	VII	VIII
$J_i$	0.9	0.9	0.9	0.9	0.9	0.9	0.9	0.9
$J_{50}$	4.3-6.9	4.3-6.9	5.3-6.9	5.3-6.9	5.3-6.9	5.3-6.9	5.3-6.9	5.3-6.9
$J_{inst}$	4.8-7.6	4.8-7.6	7.2-15	7.2-15	7.2-15	7.2-15	8.5-30	8.5-30

Considering the conditions used in this study, the data presented shows that EPFM always produces the most liberal and realistic results over LEFM, regardless of the adopted failure criterion.

In EPFM analysis the predictions from the crack initiation criterion  $J_i$  are very conservative (besides allowing as much as 0.9 mm of crack extension) when compared to those from  $J_{50}$  and, of course, from  $J_{inst}$ .  $J_{50}$  predictions are excellent when compared to  $J_{inst}$  results, which define the ductile instability event. Despite the very high ratios  $J_{inst} / J_{50}$ , their failure predictions (in terms of pressure and strains) are often close due to basically the low strain-hardening capacity exhibited by the A508-3A steel at 175°C, as evidenced by the low ratio  $S_U / S_Y$  of this material.  $J_{50}$  has produced just slightly conservative failure predictions, particularly for the surface cracks with modest dimensions and specially for the internal cracks, even the largest ones. On these bases, the relevance of  $J_{50}$  as a safe design and service criterion is ratified for internally pressurized nuclear components.

As can be seen, the failure predictions ranges in terms of ductile crack growth ( $\Delta a$ ), as well as of pressure ( $P$ ) and strains ( $e_M$ ), related to the  $J_{inst}$  criterion are too extensive as a consequence of the poor strain-hardening features of the material, which, in turn, is directly reflected on J-R curve shape. This way,  $J_{50}$  reaffirms its advantage over  $J_{inst}$  as a design and assessment criterion.

The linear extrapolation of  $J-T_{MAT}$  data from the  $\omega$  criterion for Deformation-J controlling crack growth, has provided very good J values instability estimates, as compared to those obtained from the non-linear extrapolation through the power law fit, particularly for the smallest surface cracks and once again for the internal ones.

From the data it can be assured that surface cracks are much more critical than embedded ones having the same depth and length.

Also, it is shown that crack depth has much more influence on failure predictions, for both LEFM and EPFM, than does the crack length. In fact, the later has produced only small effects over the results.

For the least critical cracks, the smallest internal ones, the trend on approaching between LEFM and EPFM failure predictions was noticed. In these cases large plasticity effects are expected, which are quite beyond the LEFM premises. Therefore, its predictions should be considered absolutely inconsistent.

As can be noted from the expected ductile crack growth levels before the vessel instability, leak-before-break is prone to occur for the most critical cracks (the deeper ones), while for the other cracks ductile instability can be established without any prior notice.

Finally it can be observed that logarithmic fit of J-R curves produces conservative failure predictions when plotted in a J-T format ( $J-T_{MAT}$  curve), and in this sense it is thought to be the optimum adjustment practice instead of power law.

## CONCLUSIONS

1 - Under upper-shelf conditions, the EPFM approach always produces more realistic (and liberal) failure predictions than does the LEFM (this one as imposed by ASME code), regardless the adopted failure criterion. In addition, less massive specimens always produce more conservative results, for both LEFM and EPFM, proving the safeness of periodical structural integrity assessments of PWR plants by using small scale testpieces.

2 - Crack initiation  $J_i$  failure predictions are highly conservative.  $J_{50}$  has produced excellent, slightly conservative, approximations of the conditions in which the real failure of the component is verified as defined by  $J_{inst}$ . Consequently,  $J_{50}$  is here ratified as an accurate criterion for safe design and service in nuclear power components industry. Ductile crack growth, internal pressure and wall strain are trustworthy parameters on instability predictions

provided  $J_{50}$  is the selected design and service criterion.

3 - Non-linear extrapolation on J-T space, adjusting  $J-T_{MAT}$  data with a power law curve, led to much closer results to those acquired from the linear extrapolation following  $\omega = 5$ .

4 - The approximations between  $J_{50}$  and  $J_{inst}$  results and from the linear and non-linear extrapolation of  $J-T_{MAT}$  data are much finer for less deep cracks (more likely to occur between periodical plant inspection programs), specially for the embedded ones.

5 - Surface cracks are much more critical than the internal ones having the same depth and length.

6 - Instability results are highly affected by crack depth changes but just slightly by changes on its length ( $l$ ); crack length has no effect over the instability results for small embedded cracks.

7 - Ductile crack extension related to initiation J ( $J_i$ ), as graphically determined, was approximately 0.9 mm instead the expected 0.2 mm; the reason for such discrepancy was the expressible steepness of J-R curve in the vicinity of its intersection with the 0.2 mm off-set line.

8 - Logarithmic fit is more effective than power law on adjusting J-R curve data points for large crack extension (where saturation-J is developed), producing conservative failure predictions through J-T diagram methodology.

9 - LEFM is inappropriate when dealing with small embedded cracks analysis under upper-shelf conditions.

10 - The larger the crack is, the greater the probability of leak-before-ductile instability. In this sense deeper cracks (in principle the most critical ones) are subject to crack arrest events as well as visual detection of the failure threshold, while the shallow ones may grow catastrophically without any prior notice.

11 - 20% side-grooving of J specimen gross thickness in both 1T and 2T specimen sizes is the ideal level for producing straight crack fronts, since 21% side-grooving always produced slightly inverted tunneling.

*Acknowledgement:* The authors gratefully acknowledge the financial support from the Fundacao para o Amparo a Pesquisa do Estado de Sao Paulo (Procs. 91/3925-4 and 91/5010-3).

## REFERENCES

- American Society of Mechanical Engineers (ASME) (1992). *Rules for in-service inspection of nuclear power plant components*. section XI, appendix A. Analysis of flaws, pp.379-399 and appendix G. Fracture toughness criteria for protection against failure, pp.437-445. ASME, New York.
- American Society for Testing and Materials (ASTM) (1995). *Annual book of ASTM standards*. v.03.01, section 3 - E1152-87. ASTM, Philadelphia.
- American Society for Testing and Materials (ASTM) (1995). *Annual book of ASTM standards*. v.03.01, section 3 - E813-89. ASTM, Philadelphia.
- American Society for Testing and Materials (ASTM) (1995). *Annual book of ASTM standards*. v.03.01, section 3 - E399-90. ASTM, Philadelphia.
- Paris, P. C. and R. E. Johnson (1983). A method of application of elastic-plastic fracture mechanics to nuclear vessels analysis, elastic-plastic fracture. *In: Symposium on fracture resistance curves and engineering applications*. (C. F. Shih and J. P. Gudas, eds.), Vol. II, pp.5-40. ASTM, Philadelphia. (ASTM-STP 803).
- Reese, E. D. and K. -H. Schwalbe (1993). The linear normalization technique - an alternative procedure for determining J-R curves from single specimen test record based on Landes' normalization method. *Fatigue and Fracture of Engineering Materials and Structures*, 16, 271-280.